

## Undifferentiated form-function

GUNJI, yukio<sup>1\*</sup>

<sup>1</sup>Faculty of Science, Kobe University

Any biological system embody complementarity between parts and whole in organized unity. Clear separation of parts and whole and complementarity, however, are not given in advance. They are gradually generated and are self-organized due to the undifferentiated feature of form and function in material. Building blocks can lead to an organized unity only if they are manipulated by a kid who can arrange the blocks. They cannot entail such unity otherwise. This fact shows that "block" containing materialistic agent who can detect and sense its own environment can self-organize the complementarity between parts and whole.

With respect to the origin of life, we have to accept the intelligence inherited in materialistic nature in a broad sense. Although this kind of proto-intelligence is different from human intelligence by which individualized objects and/or signs can be manipulated and operated, the proto-intelligence in material has capability to detect environments and generate relations to the environments simultaneously. The proto-intelligence is not explicitly found. We have to evoke and enforce proto-intelligence in the experimental setup of the origin of life. For this purpose, I will show what is and how is proto-intelligence in various biological systems, e.g., swarm of soldier crabs, *Mictyris guinotae*, navigation of garden ant, *Lasius niger* and positional information in morphogenesis.

In a system with proto-intelligence, external perturbation always detected can positively contribute to generation of orders due to the negotiation between a system and environments, resulting from proto-intelligence. I will show proto-intelligence can be implemented by asynchronous updating and mutual anticipation in our model scheme.

Keywords: origin of life, part and whole, swarm, navigation, sensing

## Two sites of life system on the Earth

MARUYAMA, Shigenori<sup>1\*</sup>

<sup>1</sup>Tokyo Institute of Technology

### Abstract

Life is a phenomenon occurring only in the space of water-rock interactions driven by magma underneath or surface material circulation driven on the top by Sun.

### Nutrient supply

Life cannot be synthesized and sustained by only water and CO (CO<sub>2</sub>). Moreover, nutrients are necessary such as P, Fe, Ca, K and others, in addition to N. Most nutrients are concentrated into the final residue of fractionated magma ocean, hence nearly absent in mantle peridotite or chondritic meteorites.

Furthermore, the life is a metasomatic phenomenon possible only in the space of water-rock interaction where both material (nutrients and water) and energy are supplied constant. If they are stopped, life stops to die immediately.

It is noteworthy to point out that the size of nutrient supply on the surface system is more than 10<sup>6</sup> times bigger than the mid-oceanic hydrothermal system.

### Subground ecosystem

Recently the idea of subground ecosystem has been proposed as an independent third life system. Subground hydrothermal system is right such as mid-oceanic ridge and as hotspot, because of the steady-state supply of magma underneath, but not in general because of absence of material circulation of nutrients and thermal and chemical energy.

### History

Under the extreme environment right after the birth of consolidation of magma ocean, UV could have been eight times higher than today. First life was not possibly synthesized near the surface, but in the deep-sea hydrothermal system, presumably in the Hadean time. Emergence of huge landmass was 800-500Ma, by the return-flow of seawater into mantle as documented by the appearance of high-P/T regional metamorphic belts along the subduction zone. This was the timing of extensive enlargement of life system using the driving force of Sun, and the golden time of life on this planet. After the establishment of the surface ecosystem, metazoan and evolved bacteria invaded the deep-sea hydrothermal system.

## Formation of iron-sulfur clusters from amino acids with pyrrhotite in aqueous solutions

OHARA, Shohei<sup>1\*</sup>, BOCTOR, Nabil Z.<sup>1</sup>, CODY, George D.<sup>1</sup>

<sup>1</sup>Geophysical Laboratory, Carnegie Institution of Washington

Iron-sulfur (Fe-S) clusters are agents that affect many biochemical processes as they are the active sites in relatively small proteins with molecular weights of 6,000 to 12,000. They are common to most ancient components of living matter and are present in a host of other organisms such as photosynthetic organisms, nitrogen-fixing bacteria, and submitochondrial fractions of mammalian origin [1]. The chemically simplest Fe-S clusters are the rhombic [2Fe-2S] and the cubane [4Fe-4S] types, and are usually integrated into proteins through coordination of the iron ions by cysteine or histidine residues. Interestingly, these biological Fe-S clusters resemble the iron sulfide minerals such as mackinawite ( $\text{Fe}_{(1+x)}\text{S}$ ) and greigite ( $\text{Fe}_3\text{S}_4$ ), which have been assigned an important role in the geochemical theory of the origins of life [2].

Cody *et al.* [3] reported the formation of carbonylated Fe-S species in the aqueous formic acid with nonanethiol and synthesized troilite (FeS) under hydrothermal conditions. They identified the carbonylated Fe-S species by UV-visible light and Raman spectroscopy. Here, we describe the results of the separation and identification of ferredoxins-like Fe-S clusters in amino acid aqueous solutions with pyrrhotite ( $\text{Fe}_{(1-x)}\text{S}$ ) by using liquid chromatography-mass spectrometry (LC-MS).

Our experiments were run in glass vials charged with amino acid containing aqueous solutions and laboratory synthesized pyrrhotite ( $\text{Fe}_{(1-x)}\text{S}$ ). Separation and identification of FeS clusters were performed with the use of ultra-performance liquid-chromatography (UPLC) coupled to UV spectroscopy and electrospray ionization-mass spectrometry (ESI-MS) detection (ACQUITY UPLC and TQD system, Waters).

Serine aqueous solution with pyrrhotite recovered from the reaction show clear yellow color. UV and ESI-MS spectra of the colored solution reveal the formation of Fe-S clusters, very similar to [2Fe-2S] and [4Fe-4S] units of ferredoxins. Proteins that contain ferredoxins are smaller than most other enzymes, having only 55 amino acid units, therefore, have been thought by some to be the most primitive enzymes [4].

Amino acids that include serine have been synthesized under hydrothermal conditions [5]. Pyrrhotite is one of the abundant sulfide minerals around sea-floor hydrothermal systems. The facile synthesis of ferredoxins-like Fe-S clusters from amino acid aqueous solutions with pyrrhotite in the present experiments suggests that these potentially catalytic species will form in natural settings, where reduced hydrothermal fluids with abiotic amino acids pass through metal sulfides-containing ore deposits. Our results lend support to the theory that the Hadean sea-floor hydrothermal systems could have provided an environment for the chemical evolution promoted by ferredoxins-like Fe-S clusters.

### Acknowledgements

We gratefully acknowledge financial support from NASA Astrobiology Institute and NASA Exobiology program.

### References

- [1] H. Beinert, R. H. Holm, E. Munck, *Science* **277**, 653 (1997).
- [2] M. J. Russell and W. Martin, *Trends Biochem. Sci.* **29**, 358 (2004).
- [3] G. D. Cody *et al.*, *Science* **289**, 1337 (2000).
- [4] R. V. Eck and M. O. Dayhoff, *Science* **152**, 363 (1966).
- [5] C. Huber and G. Wachtershauser, *Science* **314**, 630 (2006).

Keywords: iron-sulfur cluster, ferredoxin, iron sulfide mineral, amino acid, LC-ESI-MS

## Southern Mariana Forearc: geology and chemosynthetic biological community of a serpentinite terrain

OHARA, Yasuhiko<sup>1\*</sup>, REAGAN, Mark<sup>2</sup>, FUJIKURA, Katsunori<sup>3</sup>, WATANABE, Hiromi<sup>3</sup>, MICHIBAYASHI, Katsuyoshi<sup>4</sup>, ISHII, Teruaki<sup>5</sup>, STERN, Robert<sup>6</sup>, Fernando Martinez<sup>7</sup>, Katherine Kelley<sup>8</sup>

<sup>1</sup>Hydrographic and Oceanographic Department of Japan, <sup>2</sup>University of Iowa, <sup>3</sup>Japan Agency for Marine-Earth Science and Technology, <sup>4</sup>Shizuoka University, <sup>5</sup>Fukuda Geological Institute, <sup>6</sup>University of Texas at Dallas, <sup>7</sup>University of Hawaii, <sup>8</sup>University of Rhode Island

It has been considered that the hydrogen formation and the resultant abiotic formation of methane in serpentinite-hosted hydrothermal systems may have played important roles in the emergence of life on the Earth, and may have astrobiological implications for the presence of life on other planets and solar systems. Cold seeps and hydrothermal vents associated with serpentinitized mantle have been known for 15 years. In 1997, an alkaline cold seep associated with Bathymodiolus mussel communities was discovered from the South Chamorro Seamount (a serpentinite mud volcano) in the Mariana forearc. In 2001, a serpentinite-hosted, low-temperature, alkaline hydrothermal system, the Lost City hydrothermal field, was discovered along the Mid-Atlantic Ridge. In September 2010, the YK10-12 cruise with Shinkai 6500 discovered chemosynthetic biological communities (principally vesicomyid clams) that feed on serpentinitized peridotite in the southern Mariana forearc. Here we report the background and overview of the discovery.

A number of serpentinite mud volcanoes exist in the northern Mariana forearc, however none is known from the southern Mariana forearc, which faces the Challenger Deep. Instead, serpentinitized peridotite crops out extensively in the inner trench slope there, forming a serpentinite terrain. The peridotite there includes amphibole and high-temperature type serpentine (i.e., antigorite) as well as low-temperature type serpentine (i.e., chrysotile and/or lizardite). Since antigorite is rarely reported from abyssal peridotite, the southern Mariana forearc provides an important opportunity to study a different style of peridotite serpentinitization. The YK10-12 cruise was designed to study unmapped regions of the southern Mariana forearc.

Abundant chemosynthetic communities, principally consisting of vesicomyid clams, associated with serpentinitized peridotite were discovered during Shinkai 6500 dive #1234 (observer: T. Ishii) in the southern Mariana forearc, about 80 km northeast of the Challenger Deep. More than 30 live vesicomyid clams were collected, along with serpentinitized peridotite, subordinate gabbro and a fragment of a potential vent chimney. Although no active fluid venting was observed, it is likely that fluids responsible for nourishing the communities come from cold seeps associated with serpentinitization. We therefore named our discovery the Shinkai Seep Field (SSF).

This is the first description of vesicomyid clams anywhere in the Mariana forearc. Furthermore, the SSF vesicomyid clam community is the first live example described from a low-temperature serpentinite-hosted hydrothermal system from either convergent or divergent plate margins. The SSF vesicomyid clam is likely a new species, closely related genetically to the vesicomyid clam described from the high-temperature serpentinite and gabbro-hosted Logatchev hydrothermal field.

Serpentinite-hosted hydrothermal systems are thought to be unable to sustain high-biomass communities, based on the small-biomass communities observed at the Lost City hydrothermal field. However, the SSF vesicomyid clam communities are probably larger than those reported from the Nankai Trough and/or Sagami Trough, demonstrating that these serpentinite-hosted low-temperature systems can sustain high-biomass communities.

The SSF is a new class of seep system hosted by exposed upper mantle. The deep geology of the southern Mariana forearc is dominated by peridotite and is heavily faulted, suggesting that more SSF-type seeps exist in this region. Similar vents may also exist in other convergent margins like the Tonga forearc where extensive peridotite exposures in the inner trench wall also are known. Our discovery supports the prediction that serpentinite-hosted vents are widespread on the ocean floor. We hope to return to the SSF to better understand the workings of this natural laboratory as soon as possible.

Keywords: serpentinite, peridotite, upper mantle, chemosynthetic community, vesicomyid clam, Shinkai Seep Field

## Development in the early Archean of the modern-styled geochemical cycles of Fe & U through the crust-ocean-mantle system

OHMOTO, Hiroshi<sup>1\*</sup>, David C. Bevacqua<sup>1</sup>, Masamichi Hoashi<sup>1</sup>, Yumiko Watanabe<sup>1</sup>

<sup>1</sup>NASA Astrobiology Institute and Department of Geosciences, Penn State University, <sup>2</sup>NASA Astrobiology Institute and Department of Geosciences, Penn State University

Modern oceans are U-rich but Fe-poor, because U is leached from, but Fe is retained in, rocks during weathering under an oxygenated atmosphere. The oceanic U is removed by three major processes: (1) co-precipitation with carbonates in shallow seas (~60%); (2) adsorption/reduction by carbonaceous matter in black shales, which deposited in euxinic basins (~20%); and (3) adsorption by Fe<sup>III</sup>-(hydr)oxides that formed in submarine hydrothermal systems on mid-ocean ridges (MORs) (~20%). Many researchers have assumed that before ~2.4 Ga, the oceans were Fe-rich but U-poor, because the atmosphere was presumably reducing.

Here we report the results of our investigations on ~3.46 Ga jaspers (low-grade oxide-type BIFs) and associated submarine basalts from ABDP #1 drill hole at Marble Bar, Pilbara, Western Australia. These samples exhibit the mineralogical and geochemical characteristics that are essentially identical to those of jaspers and hydrothermally-altered basalts on modern ocean floors, including: (a) enrichments of Fe(III) as ferric (hydr)oxides; (b) enrichments of U, Mo and Li with Fe(III); (c) enrichments of Ba, Cu, Zn, Pb and Ag; (d) depletions of Ca and Sr; (e) anomalies (both positive and negative) in Ce concentrations; and (f) the <sup>206</sup>Pb/<sup>204</sup>Pb, <sup>207</sup>Pb/<sup>204</sup>Pb, <sup>208</sup>Pb/<sup>204</sup>Pb and <sup>238</sup>U/<sup>232</sup>Th ratios that significantly deviate from those of the bulk Earth. These data suggest that by ~3.5 Ga, the modern-styled geochemical cycles of the redox sensitive elements through the continental crust, oceans, oceanic crust and mantle had been established. This suggestion is further substantiated by the data on U/Th ratios and Ce anomalies in submarine volcanic rocks that are associated with volcanogenic massive sulfide deposits of 3.2-2.7 Ga in ages.

Subduction of oxidized and U-enriched oceanic crust has created the large-scale heterogeneity of the mantle since ~3.5 Gyr (or earlier), including the features known as 'the lead paradoxes' where Pb in the mantle is more radiogenic and has higher ratios of uraniumogenic Pb/thoriogenic Pb compared to Pb in the bulk Earth. Therefore, through the creation of the oxygenated atmosphere and oceans, aerobic microbes have influenced the geochemistry of the deep Earth since at least ~3.5 Ga ago.

Keywords: Archean, Pb, U, Fe, Marble Bar

## Earth's surface environments inferred from chemical sedimentary rocks deposited in a shallow ocean 3.2 billion years ago

OTAKE, Tsubasa<sup>1\*</sup>, SAKAMOTO, Yuki<sup>2</sup>, ITOH, Shoichi<sup>3</sup>, YURIMOTO, Hisayoshi<sup>3</sup>, KAKEGAWA, Takeshi<sup>2</sup>

<sup>1</sup>Institute for Geo-Resources and Environment, AIST, <sup>2</sup>Department of Earth Science, Graduate School of Science, Tohoku University, <sup>3</sup>Department of Natural History Sciences, Graduate School of Science, Hokkaido University

Geochemical data of ferruginous chemical sedimentary rocks (e.g., Banded Iron Formation: BIF) has been used for understanding the surface environments on early Earth. For example, Konhauser et al. (2011) recently argued that river waters became acidic to chemically mobilize Cr 2.48 billion years ago without involving any redox reactions, using the Cr/Ti ratios of various BIF samples throughout Precambrian era. However, comparing BIFs formed in different depositional environments is problematic since BIF that they found anomalous Cr/Ti ratios is the only one deposited from a shallow water environment in Archean BIFs. If Cr was mobilized in river waters, soluble Cr would have been precipitated in a shallow water environment. Therefore, we investigated geological, petrographic and geochemical characteristics of a newly found outcrop of ferruginous rocks in the Moodies group in the Barberton Greenstone Belt, South Africa, which has been interpreted to be deposited in a shallow ocean 3.2 billion years ago (e.g., Javaux et al., 2010). We also obtained unweathered ferruginous rocks in the Moodies group from an underground mine, and compared the characteristics of these samples. The objectives of this study are (1) to find chemical precipitates from a shallow water in the Moodies group; (2) to distinguish clastic and chemical components of the sedimentary rocks; and (3) to infer the depositional processes/environments of the chemical precipitate.

We collected 70 sedimentary rock samples of the Moodies Group. Samples were divided into Hematite-rich chert (HM group), Magnetite-rich chert/shale/sandstone (MT group) and Siderite-rich sandstone (SD group), based on the dominant Fe minerals. Samples in the HM group predominantly composed of fine-grained quartz (< 20 micro meter) and hematite (< 5 micro meter), which are interpreted to be chemical precipitates in origin. Samples in the MT group contain quartz, magnetite, siderite, ankerite, chlorite, biotite and chromite. The grain size of magnetite is much larger (20-150 micro meter) than that of hematite in the HM group. Magnetite is interpreted as a secondary mineral transformed from hematite during early diagenesis (Otake et al., 2007). Results of in situ oxygen isotope analysis by SIMS showed that magnetite in the Moodies group has similar  $\delta^{18}\text{O}$  values to those in least metamorphosed BIFs. All chromite observed in the MT group is overgrown by magnetite. Samples in the SD group contain quartz, siderite, chlorite, biotite, and chromite. Chromite in the SD group is included in Mg-rich siderite or silicate minerals (e.g., chlorite and biotite). Oxygen isotope compositions of chromite indicate that chromite in both MT group and SD groups was hydrothermally altered.

Results of geochemical analyses of the bulk outcrop samples showed that  $\text{Fe}_{\text{Total}}/\text{Ti}$  and  $\text{Cr}/\text{Ti}$  ratios of outcrop samples increase concordantly in the ferruginous zone, particularly in the MT group. The  $\text{Cr}/\text{Ti}$  ratios of the underground samples also increase with increasing the  $\text{Fe}_{\text{Total}}/\text{Ti}$  ratios. On the other hand, Th/U ratios of the underground samples decrease with increasing with the  $\text{Fe}_{\text{Total}}/\text{Ti}$  ratios. The changes in the Th/U and Cr/Ti require the oxidation of U and Cr to decouple geochemical behaviors of U and Cr relative to Th and Ti, respectively. The correlations of  $\text{Fe}_{\text{Total}}/\text{Ti}$  ratios with U/Th and Cr/Ti ratios indicate that dissolved Cr and U species in ocean were coprecipitated with ferric (hydr)oxides during the formation of ferruginous rocks. These results suggest that a part of shallow ocean was oxygenated -3.2 Ga, containing oxidized Cr and U species, and that ferric (hydr)oxides were precipitated due to the oxidation of dissolved ferrous iron by molecular oxygen.

### References

- Konhauser, K.O. et al., Nature 478, 369-373 (2011).
- Javaux et al., Nature 463, 934-938 (2010).
- Otake et al., Earth Planet. Sci. Lett. 257, 60-70 (2007).

Keywords: banded iron formation, hematite, magnetite, chromite, redox environment

## Estimation for CO<sub>2</sub> levels in the Paleoproterozoic from paleosols

KANZAKI, Yoshiki<sup>1\*</sup>, MURAKAMI, Takashi<sup>1</sup>

<sup>1</sup>Grad. School of Science, Univ. of Tokyo

There remain uncertainties about atmospheric conditions in the early Earth, though numerous researchers have been trying hard to elucidate. The Paleoproterozoic era (especially between 2.5 and 2.0 Ga) has attracted much attentions due to intriguing oxygen rise, multiple global scale glaciation events and co-evolution of early atmosphere and organisms. The concentration of atmospheric CO<sub>2</sub> is a factor that affects the above events and surface temperature, as known as 'faint young sun paradox'. Atmospheric photochemical modeling and paleosols as geological records have given certain constraints on P<sub>CO2</sub> levels, but some of them conflict with one another (e.g., less than 100 PAL (meaning 100 times present atmospheric level) at ~ 2.2Ga (Rye et al., 1995); 7 - 70 PAL at 2.5 - 1.8 Ga (Sheldon, 2006); more than 100 PAL at 2.8Ga (Haqq-Misra et al., 2008)). To estimate the most likely P<sub>CO2</sub> levels in the Paleoproterozoic, paleosols constraints must be re-evaluated.

We used the data of the Cooper Lake paleosol (formed at ~ 2.45Ga, from Utsunomiya et al. (2003)) as this paleosol is diagnosed as well preserved from physical erosion (Murakami et al., 2011). To extract P<sub>CO2</sub> constraints, we firstly estimated ion concentrations in pore water at steady state. Considering the mass balance between solid and water phases, the loss of elements from solid (mol/L (bulk)), which can be obtained from a paleosol, must be the same as the amount transported out from the paleosol by fluid. The amount transported can be expressed by the product of the following parameters; steady state concentrations of ions in water phase (mol/L (water)), transport rate by fluid flow (/yr), porosity of the paleosol at the time of weathering (L (water)/L (bulk)), and total weathering time (yr). Assuming dissolved Si concentration at steady state as 10<sup>-4</sup> - 10<sup>-3</sup> mol/L, Na, Mg, Ca and P concentrations in pore water in a paleosol can be obtained from this mass balance method. As for K concentration, two extreme scenarios were considered, which are no weathering of K scenario and complete weathered K scenario, because K recorded in the Cooper Lake paleosol is affected by K-metasomatism after the paleosol formation. As a next step, we calculated the pHs at which charges of pore waters are maintained, changing P<sub>CO2</sub> from 0.1 PAL to 1000 PAL. Anions considered other than carbonate species included phosphate species, concentrations of which were obtained by mass balance method from the paleosol, and Cl<sup>-</sup> assumed as non buffering anion in the range of < 0.002 M, although Cl<sup>-</sup> concentrations only caused the charge balanced pHs to shift by at most 0.3 in pH unit. As a final step, these charge-balanced waters were checked for saturation state with respect to secondary minerals, and here, kaolinite and smectite were chosen for such minerals. The calculations have revealed that 10 - 1000 PAL of CO<sub>2</sub> are the most likely levels operating at the time of the formation of the Cooper Lake paleosol for the above two extreme scenarios for K. These estimated CO<sub>2</sub> levels are not inconsistent with more than 100 PAL of P<sub>CO2</sub> at 2.8 Ga estimated from atmospheric photochemical modeling (Haqq-Misra et al., 2008).

Keywords: paleosol, weathering, faint young sun paradox, carbon dioxide, Paleoproterozoic

## Nitrogen cycles in hadopelagic sediments

NUNOURA, Takuro<sup>1\*</sup>, NISHIZAWA, Manabu<sup>2</sup>, KIKUCHI, Tohru<sup>3</sup>, HIRAI, Miho<sup>1</sup>, MIYAZAKI, Junichi<sup>2</sup>, KOBA, Keisuke<sup>4</sup>, TAKAI, Ken<sup>1</sup>

<sup>1</sup>Extremobiosphere Research Program, JAMSTEC, <sup>2</sup>Precambrian Ecosystem Laboratory, JAMSTEC, <sup>3</sup>International College of Arts & Sciences, Yokohama City University, <sup>4</sup>Faculty of Agriculture, Tokyo University of Agriculture & Technology

Nitrogen cycle in deep-sea sediments is still uncertain while that in the aphotic oceanic water has intensively been investigated. A hadopelagic sediment core (1.1m in length) was taken by the ROV ABISMO from the Ogasawara Trench at a depth of 9760m. Interstitial water chemistry indicates that nitrate reduction occurred in the upper parts of the sediment core, but significant sulfate reduction did not even at the bottom of the core column. Comprehensive molecular analyses including clone analyses and quantitative PCR for SSU rRNA genes and functional genes (*amoA*, *nirK*, *hao/hzo*) present unique distribution patterns of nitrifiers, denitrifiers and anammox in the nitrate reduction zone. The maximum abundance of both aerobic nitrifiers (archaeal and proteobacterial ammonia oxidizers, and nitrite oxidizing bacteria) and proteobacterial denitrifiers occurred in a same horizon, and stable isotopic analyses for nitrate also suggest the occurrence of nitrification in the nitrate reduction zone. On the other hand, anammox population decreased with increasing depth. These results suggest that the abundance of aerobic nitrifiers is regulated by both oxygen and ammonium concentrations, and the anammox population is suppressed as a result of competition for nitrite with nitrite oxidizer and denitrifer except for surface layer in the hadopelagic sediment.

Keywords: deep-sea, sediment, nitrogen cycle, nitrification, denitrification



## Pyrite spherulites found in the Nishi Kannondo Kuroko deposit in the Hokuroku district: Comparison with Suiyo Seamount.

HASEGAWA, Miki<sup>1\*</sup>, YAMADA, Ryoichi<sup>1</sup>, KAKEGAWA, Takeshi<sup>1</sup>

<sup>1</sup>Department of EARTH SCIENCES, Graduate School of Science, Tohoku University

Pyrite spherulites are often observed in modern seafloor hydrothermal vents as well as ancient hydrothermal ore deposits. Sulfide spherulites are often considered as an important material in the origin of life by catalyzing metabolisms or acting like a cell. However, formation processes of the pyrite and their association to biotic processes are not well understood due to a lack of detailed investigations on mineralogical and geochemical characteristics of the pyrite. We found possible fossil of chimneys including much pyrite spherulites in the Nishi-Kannondo deposit which is one of Kuroko-type massive sulfide deposits Nishi Kannondo deposits generated by an ancient (~13Ma) hydrothermal system. It is located in the Hanaoka mining camp in the Hokuroku district, Akita Prefecture, Japan. The same spherules were also found in sulfide-sulfate mounds at modern submarine hydrothermal field of the Suiyo Seamount in the Izu-Bonin Arc, Western Pacific. Objectives of this study are (1) to reveal detailed mineralogical and chemical characteristics of spherulitic pyrite, and (2) to examine the relationship of the formation of spherulitic pyrite and biological activities.

In the Nishi Kannondo deposit, we collected various ore samples. Pyrite-rich ores are commonly found in the western and northern part of the ore deposit. Black ores (consist essentially of sphalerite and galena) are found in the center of the ore deposit, and barite ores are from southern side of the deposit. These lithological variations correspond to the paleo-structures of chimney and mounds. Pyrite spherulites are found in barite-rich ores which may be located at the chimney out wall or mound inside: those were formed in low temperature and sulfate-rich environments, thus in distant from black smoker activities.

Based on microscopic observations, an individual pyrite spherulite, a few mm in diameter, is divided into core, and outer envelope parts. Core parts of 134 spherulites were grouped into 3 types according to morphology and constituent minerals. The most are i) multiple sulfide microcrystal type (69%, e.g., pyrite and tennantite), ii) pit or porous type (22%), and iii) sulfide single crystal type (9%, e.g., pyrite and tennantite) to the least. The pit or porous type is associated with pyrite, covellite, quartz and organic carbon (TOC ~ 0.1wt%) around the pit. Outer envelope parts are composed of radial pyrite crystals, and some have concentric layers with other minor minerals (e.g., chalcopyrite, tennantite and molybdenite). In chemical mapping of the pyrite layers, concentric zonings of As and Cu were observed. These characteristics of outer envelope parts of the pyrite spherulites indicate that the pyrites record periodical precipitation processes, which occur rapidly or slowly. We also propose that these differences of characteristics of core and outer envelope parts reflect changes in surrounding environments during the formation of pyrite spherulites, such as periodic discharge of "hot" hydrothermal fluids. Some pit or porous types contain organic matter. However, it is still uncertain if microbial activities initiated spherulite formations.

At the Suiyo seamount, black smokers are actively discharging, resulting the formation of large sulfide mounds on the seafloor. We collected various samples different in the formation phase, such as a freshly-formed chimney and aged sulfide mounds. Based on microscopic observations, spherulites are recognized in the matrix comprising barite, similar to that of Nishi Kannondo deposit. An individual spherulite, a few mm in diameter, consists essentially of pyrite and sphalerite. Those suggest to be performing similar process in case of the Nishi-Kannondo deposit.

Keywords: pyrite, spherulite, concentric layer, sulfide microcrystal, organic matter

## Size distribution of ferrihydrite aggregate and its effects on metal adsorption and transport

TSUBAKI, Haruka<sup>1\*</sup>, Takumi Saito<sup>2</sup>, MURAKAMI, Takashi<sup>1</sup>

<sup>1</sup>Dept. Earth & Planet. Sci., Univ. Tokyo, <sup>2</sup>Dept. Nucl. Eng. & Manage., Univ. Tokyo

Ferrihydrite, iron oxyhydroxide nanomineral (< ~ 100 nm in size), is ubiquitous on the surface of the Earth. Ferrihydrite has a large capacity to adsorb heavy metals in solutions because of its large specific surface area. The adsorbed metals onto ferrihydrite are transported in ground and river waters, affecting the redistribution of the metals in surface environments. Ferrihydrite forms aggregates with various sizes and this can affect the uptake behavior of heavy metals and the subsequent transport. Furthermore, filtration with 450- or 220-nm pore, which is the most frequently used to physically separate ferrihydrite in adsorption measurements, can give incorrect concentrations of adsorbates because of the extremely small size of ferrihydrite primary particles.

For the present study, ferrihydrite was investigated by various methods to understand the size distribution and the influence of metal adsorption on the size distribution, and then a possible impact on the transport of adsorbed metals was discussed. Size distribution of ferrihydrite and its aggregates were examined by gravitational settling, centrifugation, dynamic light scattering and transmission electron microscopy (TEM). Adsorption experiments of Zn at acidic to neutral pH were performed with ferrihydrite of various concentrations.

Direct observation by TEM revealed that individual, spherical ferrihydrite nanomineral of ~ 5 nm was indeed present, but they formed aggregates of around 100 nm. Meanwhile, the other methods for size distribution indicated that suspended ferrihydrite in solution formed aggregates of several tens of nm to a few tens of microns. The size distribution varied with pH and Fe concentration; smaller aggregates were formed at lower pH and lower Fe concentration. Despite the size distribution, most aggregates did not pass through filters with 450-nm pore.

The amounts of Zn adsorbed on ferrihydrite were measured for solutions with aggregates fractionated by size, and then, they were calculated on the assumption that the adsorption occurred on the surface of individual 5-nm ferrihydrite nanominerals. Good agreement between the measured and calculated amounts of Zn suggests that the structures of the aggregates are loose enough for Zn ions to diffuse into the aggregates and reach to individual nanominerals. It turned out that conventional adsorption experiments with relatively high Fe concentrations could describe metal adsorption almost correctly.

Sedimentation of particles depends on the size, in general; it takes about ten days for ferrihydrite aggregates of 100 nm in diameter to settle down on the bottom of solution of 10 mm height. This implies that heavy metals adsorbed on the aggregates with 100 nm or larger sizes are not transported further in water systems, whereas those on smaller aggregates are transported further.

Keywords: nanominerals, heavy metals, adsorption, aggregate size, transport

## The adsorption behavior on montmorillonite under hydrothermal condition

MIZUNO, Yuki<sup>1\*</sup>, FUCHIDA, Shigeshi<sup>1</sup>, MASUDA, Harue<sup>1</sup>

<sup>1</sup>Osaka City University

Amino acids comprising proteins are the most fundamental substances of life. Stability and polymerization of amino acids are essentially important to succeed the life on the primitive earth. Thermal energy of submarine hydrothermal systems might be the driving force of amino acid polymerization, although the amino acids can easily be decomposed by heat. Clay minerals in the system would protect the amino acids from thermal decomposition (Imai, 2004). In this study, the role of clay minerals to form peptides at hydrothermal condition was examined by two different approaches from the point of views of laboratory experiment.

First, 1 mmol/L glycine solution was heated with 1g montmorillonite or amorphous silica at pH 2, at which the maximum concentration of adsorbed glycine was observed at room temperature, and 150 degrees for 168 hours. After the reaction, amount of adsorbed glycine onto montmorillonite and amorphous silica were 2046 nmol/g and 307 nmol/g, respectively. The glycine concentration in the solution was the same for the solution after the reaction. Peptide formation was not observed in the set conditions.

Second, pH dependence on the peptide formation was examined. 1 mmol/L glycine solution with 1g montmorillonite was heated changing pH from 2 to 12 at 150 degrees for 168 hours. The glycine adsorbed was 101.54 nmol/g, 76.65 nmol/g, 88.56 nmol/g, 46.47nmol/g, 48.87nmol/g, and 28.50nmol/g at pH 2, 4, 6, 8, 10 and 12, respectively. In the solution, remaining glycine was 0.74 mmol/L, 0.42mmol/L, 0.40mmol/L, 0.54mmol/L, 0.80mmol/L, 0.80mmol/L at pH 2, 4, 6, 8, 10 and 12, respectively. Peptide was not observed in the series of this experiments, similar to the results of above experiment. Since the glycine is dominant cation below pH 5.97 (isoelectric point) and surface of montmorillonite is charged negative, the montmorillonite adsorbs glycine easily in the acidic solution below that pH. The remaining amount of glycine is small at around neutral pH, probably because the glycine is nonpolar molecule which has small affinity to be adsorbed.

Those experiments suggest that the montmorillonite preserves more glycine via adsorption at acidic condition in high temperature hydrothermal solution. Montmorillonite may maintain the stability of glycine in the solution at around neutral pH. Peptide formation was not observed at any conditions of this study. Since the peptide formation is dehydration reaction, it would rarely occur in the aqueous solution. Thus, the peptide formation would be favorable under dry conditions. Thus, the clay minerals would work to condense the amino acid, and dry condition would be needed for further reaction for peptide formation.

Keywords: hydrothermal condition, glycine, montmorillonite, adsorption, pH

## Reduction and oxidation in natural waters and in water in creatures -Breaking the spell of Sillen's pE concept-

NAKAMURA, Ko-ichi<sup>1\*</sup>

<sup>1</sup>National Institute of Advanced Industrial Science and Technology (AIST)

The pE of natural water or water in biology cannot be measured, hence it is impractical concept. The 20th century was the century that almost all textbooks put the equilibrium concept as a principal rule. To progress our research in the complexity of advanced scientific disciplines we need to have tendencies to think kinematically.

- [1] LG Sillen (1959) Graphic presentation of equilibrium data. in Kholthoff & Elving eds., *Treatise on analytical chemistry, Pt. 1, v.1*, 277-317. The Chem. Soc. (1964) *Stability constants of metal-ion complexes, Sp. Pub. 17*.
- [2] W Stumm & JJ Morgan (1970, 1981, 1996) *Aquatic chemistry*. W Stumm (1978) What is the pE of the sea? *Thalassia Jugoslavica*, 14, 197-208. W Stumm (1984) Interpretation and measurement of redox intensity in natural waters. *Schweiz. Z. Hydrol.* 46, 291-296. AJB Zhender & W Stumm (1988) Geochemistry and biogeochemistry of anaerobic habitats. in Zhender ed., *Biology of anaerobic microorganisms*, p.1-38.
- [3] AH Truesdell (1968) The advantage of using pE rather than Eh in redox equilibrium calculations. *J Geol. Educ.*, 16, 17-20. FMM Morel & JG Hering (1983, 1993) *Principles (and applications) of aquatic chemistry*. JF Pankow (1991) *Aquatic chemistry concepts*. The Chem. Soc. (1971) *Stability constants of metal-ion complexes, Supplement No.1, Sp. Pub. 25*. R Parsons (1975) The role of oxygen in redox processes in aqueous solutions. in ED Goldberg ed., *The nature of seawater, Dahlem workshop*, 505-522. R Parsons (1978) Discussion. *Thalassia Jugoslavica*, 14, 207.
- [5] RD Lindberg & DD Runnells (1984) Groundwater redox reactions: An analysis of equilibrium state applied to Eh measurements and geochemical modeling. *Science* 225, 925-927. D Langmuir (1997) *Aqueous environmental geochemistry*. Ch. 11.1.
- [6] W Stumm (1967) Redox potential as an environmental parameter: conceptual significance and operational limitation. in O Jagg & H Liebmann, eds., *Advances in water pollution research*, 1, 283-308. JN Butler (1998) *Ionic equilibrium*, Ch. 9.
- [9] RJ Silbey, RA Alberty & MG Bawendi (2005) *Physical Chemistry*, Ch. 5.11. WR Smith & RW Missen (1982, 1991) *Chemical reactions equilibrium analysis*.
- [10] E.g., J Buffle (1988) *Complexation reactions in aquatic systems - an analytical approach*. DA Dzombak & FMM Morel (1989) *Surface complexation modeling - Hydrous ferric oxide*.
- [11] H Taube (1970) *Electron transfer reactions of complex ions in solution*. Ch. 3, ABP Lever (1990) *Inorg. Chem.*, 29, 1271-1285. G Lappin (1999) *Redox mechanisms in inorganic chemistry*. Ch.1, Table 1.4. ML Tobe & J Burgess (1999) *Inorganic reaction mechanisms*. Ch. 9, Fig. 9.23, L Perrin et al. (2001) *Inorg. Chem.*, 40, 5806-5811.
- [12] E.g., RH Holm et al. (1996) Structural and functional aspects of metal sites in biology. *Chem. Rev.*, 96, 2239-2314.
- [13] E.g., SA Bennett et al. (2008) *Earth Planet. Sci. Lett.*, 270, 157-167. BM Toner et al. (2009) *Nature Geosci.*, 2, 197-201.
- [14] J Li et al. (1996) *Inorg. Chem.*, 35, 4694-4702. M Undesemaa & T Tamm (2003) *J. Phys. Chem. A*, 107, 9997-10003, CJ Cramer & DG Truhler (2009) *Phys. Chem. Chem. Phys.*, 11, 10757-10816.
- [15] J Buffle & G Horvai eds. (2000) *In Situ monitoring of aquatic systems*. RG Compton & CE Banks (2007, 2011) *Understanding voltammetry*. Rev. ed.
- [16] A Warshel et al. (2006) *Biochim. Biophys. Acta*, 1764, 1647-1676. E.g., J Mao et al. (2003) How Cytochromes with different folds control Heme redox potentials. *Biochem.* 42, 9829-9840.
- [18] TL Hill (1985) *Cooperativity theory in biochemistry*.
- [19] KG Denbigh (1951) *The thermodynamics of the steady state*. KG Denbigh (1981) *The principles of chemical equilibrium*, 4th ed., See p.5. KG Denbigh & JCR Turner (1984) *Chemical reactor theory: an introduction*, 3rd ed.
- [20] C Godreche, ed. (1991) *Solids Far from Equilibrium*. JW Mullin (2001) *Crystallization*, 4th ed. J Wang (2006) *Analytical electrochemistry*, 3rd ed. DA Beard & H Qian (2008) *Chemical Biophysics.*, JJR Frausto da Silva & RJP Williams (2001) *The biological chemistry of the elements*, 2nd ed.

Keywords: reduction and oxidation potential, mixed potential, hydration, equilibrium, kinetics

## Enrichment mechanisms of tellurium in ferromanganese crusts

Toshiki Sugiyama<sup>1</sup>, SAKAGUCHI, Aya<sup>1\*</sup>, KASHIWABARA, Teruhiko<sup>2</sup>, USUI, Akira<sup>3</sup>, TAKAHASHI, Yoshio<sup>1</sup>

<sup>1</sup>Department of Earth and Planetary Systems Science, Hiroshima University, <sup>2</sup>Japan Agency for Marine-Earth Science and Technology, <sup>3</sup>Department of Natural Environmental Science, Faculty of Science, Kochi University

Marine ferromanganese crusts (FMCs) consist of iron (Fe) hydroxides and manganese (Mn) oxides with various minor and trace elements. Especially for tellurium (Te), which is recognized as one of the rare metals, it has been reported that this element is concentrated about 105 times in FMCs compared with earth's crust, and the host phase might be Fe (oxy)hydroxide (Hein et al., 2003). Actually, in our previous study, the high concentration of Te in very surface layers of FMCs was found from the top to halfway down of a seamount in the Pacific Ocean. However, the concentration of Te in surface layers through the seamount showed good correlation with that of Mn instead of Fe. In this study, we attempted to clarify the enrichment mechanism of Te in FMCs with some methods including X-ray absorption fine structure (XAFS) technique for synthesised/natural samples.

Seventeen FMC samples were collected from the Takuyo-Daigo seamount, from 950 m (summit) to 3000 m in water depth, with hyper-dolphin (remotely operated vehicle) equipped with live video camera and manipulators. The growth rates of all FMC samples were estimated to be about 3 mm/Ma. Very surface layer (less than 1 mm) of all FMC was analyzed with XRD and XAFS to confirm the mineral composition and speciation of Te. Furthermore, to serve as an aid to clarify the adsorption mechanism of Te on FMCs, distribution coefficients (Kd) and oxidation states were determined through the adsorption experiments of Te(IV) and Te(VI) on ferrihydrite and delta-MnO<sub>2</sub>. In all the experiments, pH and ionic strength were adjusted to pH 7.5 and 0.7 M, respectively. The oxidation state of Te in water phase was determined with HPLC-ICP-MS. As for the analysis of oxidation and adsorption states on the solid phase, XAFS was employed.

The major mineral composition of Fe and Mn had no significant variation through the water depth of Takuyo-Daigo seamount. The oxidation state of Te in all samples showed hexavalent, and there was no significant difference of adsorption state independent of the DO, salinity and temperature in water. It has been reported that Te exists as tetravalent and hexavalent in sea water of the Pacific Ocean (Lee and Edmond, 1985). Thus, it can be said that the Te in sea water is oxidised and incorporated into FMCs. As a result of the adsorption experiments in laboratory, the Kd of Te on ferrihydrite was larger than that of delta-MnO<sub>2</sub>, and Te(IV) was adsorbed to a larger degree than Te(VI) on both minerals (Fig.1 a). The adsorption experiments of Te(IV) on delta-MnO<sub>2</sub> showed that the solid phase has only hexavalent Te (Fig.1 b), although the water phase has both tetra and hexavalent species of Te. Te(IV) on ferrihydrite was not oxidized to Te(VI). From these results, it can be suggested that Te(IV) was oxidized by delta-MnO<sub>2</sub> and would be adsorbed onto ferrihydrite. Actually, the results of double-cell adsorption experiments support this hypothesis. The detail of our results and discussion will be given in the presentation.

Keywords: ferromanganese crusts, tellurium, XAFS

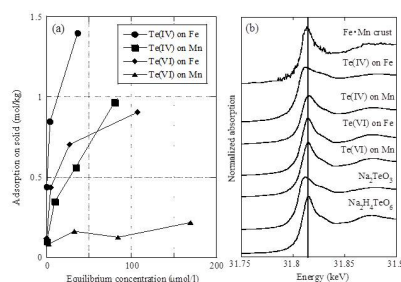


Fig.1 (a) The adsorption isotherm for Te on synthesized ferrihydrite and  $\delta$ -MnO<sub>2</sub>, and (b) the chemical species of Te in adsorbed oxides and natural ferromanganese crust

## The difference of diffusion coefficients in water for arsenic compounds at various pH and its dominant factors

TANAKA, Masato<sup>1\*</sup>, TAKAHASHI, Yoshio<sup>1</sup>, SAKAMITSU, Mika<sup>1</sup>

<sup>1</sup>Graduate School of Science, Hiroshima University

Toxicity of arsenic is significantly variable depending on its speciation and it is important to understand the migration behaviors of this speciation, where diffusion can control transport mechanism in the impermeable layer such as in the pore waters of sediments and rocks. Diffusion coefficients ( $D$ s) of arsenite, arsenate, methylarsonic acid (MMA), and phenylarsonic acid (PAA) as a function of pH were determined in this study, which contributes to the better understanding of transport of various arsenic speciation in the environment. By aid of *ab initio* molecular orbital (MO) calculations and Monte Carlo (MC) simulations, this study sheds light on the origin of pH dependence on the diffusion coefficients for the arsenic compounds.

Diffusion experiments were conducted by diffusion cell method, and  $D$ s were determined by measuring the concentrations of arsenic species every 10 minutes during the diffusion. The concentrations were measured by ICP-MS. The molar volumes and electrostatic potential maps were calculated by means of *ab initio* MO method to estimate the molecular size and the degree of polarization of arsenic compounds. Radial distribution functions of distances between arsenic and oxygen atoms in water molecule for arsenic compounds were determined by MC simulations to obtain hydration structures of arsenic species.

The  $D$ s of arsenic compounds decreased with increasing pH, and the trends were different depending on the type of compounds. With particular reference to the arsenate derivatives,  $D$  was different reflecting difference of functional groups at low pH, but  $D$  became similar at high pH even though they have different solute sizes. The molecular simulations indicate that for the neutral speciation at low pH, the diffusion is dominated not only by the molecular size but also by charge distribution in the molecule (degree of polarization). On the other hand, for the dissociated speciation at high pH, the diffusion is dominated by charged oxyanion due to high association of water molecules regardless their functional groups. This effect is common for all the arsenic species, which causes that the differences in their  $D$ s become smaller as the pH increases, especially for arsenate, MMA, and PAA.

Keywords: arsenic compound, diffusion coefficient, pH dependence, *ab initio* MO method, Monte Carlo simulation, hydration structure

## Identification and characterization of phase governing Eu(III) uptake in granite by microscopic observations

HASEGAWA, Yusuke<sup>1</sup>, FUKUSHI, Keisuke<sup>2\*</sup>, MAEDA, Koshi<sup>1</sup>, Yuhei Yamamoto<sup>3</sup>, Daisuke Aosai<sup>3</sup>, TAKASHI, Mizuno<sup>3</sup>

<sup>1</sup>Graduate School of Natural Science and Technology, <sup>2</sup>Institute of Nature and Environmental Technology, Kanazawa University,

<sup>3</sup>Japan Atomic Energy Agency

Sorption behaviors of trace elements on single mineral surface have been extensively studied. However, there have been very few researches for the trace elements sorption on complex mineral assemblages such as rocks, sediments and soils. In order to make predictions for the trace elements migration on geologic media, it is crucial to understand the molecular-scale interaction of trace elements with complex mineral assemblages, and to construct the thermodynamic sorption models based on the molecular-scale information. In the present study, the sorption of trace level of Eu(III) on complex mineral assemblages, slightly altered granite, as function of pH was studied by microscopic approaches.

The granite sample was collected from a borehole at a depth of 400m from the Mizunami Underground Research Laboratory constructed by Japan Atomic Energy Agency in central Japan. The granite sample was visually fresh. However, the microscope observation as well as the X-ray diffraction patterns of clay fraction shows that the occurrences of smectite, chlorite, vermiculate, calcite and hydrous iron oxides. The thin sections of the granite were prepared for Eu(III) sorption experiments. The thin sections were reacted for 24 hours in solutions of which pH were adjusted to 4, 5 and 6 under 0.01 M NaCl support electrolyte and analyzed by electron probe micro analyzer (EPMA). Then, the same thin sections were reacted for 24 hours in solutions of which 1.5 ppm of Eu(III) was added into solutions mentioned above. The resulting thin sections were served for observation and analyses by EPMA.

EPMA analyses of the thin sections after Eu(III) sorption shows that the Eu contents in quartz, plagioclase, K-feldspar, chlorite, calcite and iron hydroxide were less than detection limit. In contrast, smectite always contains up to 2.7 wt% of Eu. Part of biotite grains also contains up to 6.5 wt% of Eu. Because the Eu concentration in solution is 1.5 ppm, the concentrated factors of Eu in smectite and biotite are more than ten thousands. Quantitatively, the amount of smectite in the granite is negligible. We concluded that biotite is most important phase governing Eu(III) uptake on the granite. The texture of Eu enriched parts in the biotite grain were different from the original texture. The Eu enriched parts were distorted and the distinct cleavages appear. There is good negative correlation between K and Eu in the affected biotite grain. The relationship shows the uptake mode of Eu on biotite is ion-exchange of K in biotite and Eu(III) in solution. The number of the Eu affected biotite grain increases with decreasing pH. This indicates that the intercalation of Eu(III) to K in biotite favors at low pH conditions. The macroscopic sorption behavior of Eu(III) on granite (Maeda et al. this volume) is consistent with the microscopic observations.

Keywords: granite, Eu(III), sorption, biotite, EPMA

## Modeling Eu(III) sorption on granite

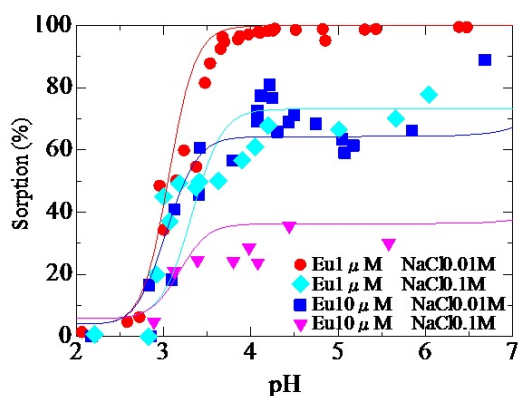
MAEDA, Koshi<sup>1\*</sup>, HASEGAWA, Yusuke<sup>1</sup>, Yuhei Yamamoto<sup>3</sup>, Daisuke Aosai<sup>3</sup>, Mizuno Takashi<sup>3</sup>, FUKUSHI, Keisuke<sup>2</sup>

<sup>1</sup>Graduate School of Natural Science and Technology, Kanazawa University, <sup>2</sup>Institute of Nature and Environmental Technology, Kanazawa University, <sup>3</sup>Japan Atomic Energy Agency

There have been very few researches for the trace elements sorption on complex mineral assemblages such as rocks, sediments and soils. In order to make predictions for the trace elements migration on geologic media, it is crucial to understand the nano-scale interaction of trace elements with complex mineral assemblages, and to construct the thermodynamic sorption models based on the molecular-scale information. In the present study, the batch sorption experiments of Eu(III) on granite were conducted as function of pH and ionic strength. The sorption behavior was modeled based on our microscopic observation (Hasegawa et al. this volume).

The granite sample was collected from a borehole at a depth of 400 m from the Mizunami Underground Research Laboratory constructed by Japan Atomic Energy Agency in central Japan. The granite was visually fresh. However, the microscope observation and the X-ray diffraction analysis of clay fraction show the occurrences of smectite, chlorite, vermiculate, calcite and hydrous iron oxides. Eu(III) sorption experiments on granite in the Teflon vessels were conducted as function of pH (2 to 8), ionic strength ( $I=0.01$  and  $0.1$ ) and Eu concentration (1 and 10  $\mu\text{M}$ ) under ultra-pure  $\text{N}_2$  atmosphere in room temperature.

The experiments and modeling results are shown in the Figure. Sorption ratio of Eu(III) was almost zero at pH 2. They abruptly increase with pH up to 3.5. Above pH 3.5, the sorption ratio indicates almost constant. The sorption strongly depends on ionic strength at the pH more than 3.5. Our microscopic observations show that Eu(III) is selectively scavenged by biotite and that sorption mode of Eu(III) is identified to be exchange reaction with inter-layer K in biotite and Eu(III). The sorption behaviors at pH more than 3.5 are consistent with the cation exchange reaction. At low pH conditions, less than pH 3.5, the release of the Al and/or Fe must occur with dissolution of minerals. The Al and/or Fe should be competed with Eu(III) on the exchange site of biotite. The sorption modeling is simply considering ion exchange reaction and solubility of hydrous iron oxide. The model reasonably reproduces the overall sorption behavior.





## Organic matrices regulating the biomineralization -Structural and functional analyses of Pif in the nacreous layer-

SUZUKI, Michio<sup>1\*</sup>, KOGURE, Toshihiro<sup>1</sup>, Hiromichi Nagasawa<sup>2</sup>

<sup>1</sup>Graduate School of Science, the University of Tokyo, <sup>2</sup>Graduate School of Agricultural and Life Sciences, the University of Tokyo

A wide variety of organisms use biominerals to generate hard tissues that function in the maintenance of body structure, protection from enemies, sensing magnetic fields and gravity, and the storage of minerals. In addition to their mineral components, biominerals contain a small amount of organic matrices that likely play important roles in biomineral formation. These organic matrices have been identified from a wide range of biominerals, such as bones, teeth, coccoliths, otoliths, the exoskeleton of crustaceans, seashells, eggshells, the exoskeleton of corals and bacterial magnetite. Acidic matrices, which are necessary for mineralization, are included in these biominerals. These acidic matrices can interact specifically with the mineral's crystal surface to induce axis-oriented nucleation, intercalate into the crystal lattice, determine the mineral phase, or function as the framework of biomineral formation.

In molluscan shells, these organic matrices play a role in the formation of calcium carbonate crystals. In turn, these crystals are necessary for the formation of the nacreous layer contained in the pearl oyster shell, which is used for production of jewelry pearls. Within the nacreous layer, aragonite calcium carbonate crystals are sandwiched between sheets of the organic matrix, and the c-axis of the crystals is perpendicular to the shell surface. Within molluscan shells, the major components of organic matrices are Asp-rich calcium-binding proteins and chitin. Previous studies suggested that unidentified acidic proteins induce aragonite formation and control the direction of the c-axis.

In 1960, Watabe and Wilbur first reported that the whole organic matrices extracted from the nacreous layer induced aragonite crystal formation. Later, it was suggested that Asp amino acid residues of the organic matrices interact with calcium atoms in the calcium carbonate to regulate its polymorph. Recent studies imply that a few organic matrices in the nacreous layer play important roles in the formation of such characteristic aragonite crystals. Although a number of matrix proteins have been identified from various mollusk shells, any fully identified proteins which induce aragonite crystal formation characteristic of nacre as mentioned above have not yet been found out, nor has any Asp-rich acidic macromolecule been discovered from the nacreous layer. Therefore, the molecular mechanism of formation of the characteristic structure of the nacreous layer remains unknown. To clarify the formation mechanism of the nacreous layer, we searched for a key molecule in the nacreous layer and identified a novel acidic matrix protein, Pif, in *P. fucata* that specifically binds to aragonite crystals. The Pif cDNA encoded a precursor protein, which gave Pif 97 and Pif 80 posttranslationally. The results of immunolocalization, a knockdown experiment by RNAi, *in vitro* calcium carbonate crystallization studies and the existences of orthologs in closely related species strongly indicated that Pif regulates the nacre formation such as stacked compartment structure, polymorph switching and crystal alignment.

Keywords: aragonite, nacreous layer, *Pinctada fucata*, matrix protein

## Composition of carbonate chemical species in the Phanerozoic ocean estimated from fossil cyanobacteria

SHIRAISHI, Fumito<sup>1\*</sup>

<sup>1</sup>Department of Earth and Planetary Systems Science, Graduate School of Science, Hiroshima University

The major ionic composition of Phanerozoic ocean has been mainly estimated from evaporates. On the other hand, there have been difficulties for estimating the carbonate chemical species due to the lack of appropriate indicator, despite that it is essential for reconstructing e.g. global carbon cycle. Although some previous studies attempted to estimate carbonate composition by applying assumptions such as constant alkalinity throughout the Phanerozoic (Royer et al. 2004, *GSA Today* 14, 4-10; Riding & Liang 2005, *Palaeo3*, 219, 101-115; Locklair & Lerman 2005, *Cham. Geol.* 217, 113-126), their results were significantly varied by applied assumptions.

The present study focused on fossil cyanobacteria as a potential indicator for the composition of carbonate species in the Phanerozoic ocean. Cyanobacteria are calcified by photosynthesis-induced  $\text{CaCO}_3$  precipitation, and its degree is considered to reflect the ambient carbonate composition. Therefore, its fossil record is expected to be a good indicator for ancient ocean carbonate composition.

For this purpose, it is necessary to clarify the chemical parameter reflecting the degree of cyanobacterial calcification. The previous studies based on simulation suggested that the parameter would be "CaCO<sub>3</sub> saturation state increased by photosynthesis" (Arp et al. 2001, *Science* 292, 1701-1704; Aloisi 2008, *GCA* 72, 6037-6060). However, actual measurements using microelectrodes revealed that the parameter should be "CaCO<sub>3</sub> saturation state achieved by photosynthesis" (Shiraishi 2012, *GCA* 77, 157-174).

Based on this finding, the composition of carbonate chemical species in the Phanerozoic ocean was calculated from fossil record of calcified cyanobacteria. Estimated range and trend are similar to those of previous studies, but exhibited more frequent changes. In a future study, it is necessary to understand the relationship between CaCO<sub>3</sub> saturation state achieved by photosynthesis and calcification amount, in order to increase the reliability of estimation.

## Stromatolitic travertines formed by cyanobacterium, *Microcoleus* sp.

OKUMURA, Tomoyo<sup>1\*</sup>

<sup>1</sup>Kyushu University

Precambrian stromatolites have been investigated over one century as important records of the early biosphere, however the detailed processes have not been specified because the initial structures and chemical features were obscured due to recrystallization, deformation, and scarcity of microfossils. Investigation of physicochemical and biological processes of modern analogs for ancient stromatolites is a potential approach for interpreting such ancient stromatolite formation. Travertines, carbonate precipitates from hot spring, have common fabrics to the ancient stromatolites in terms of sub-mm order lamination and scarcity of detrital particles and preserved microbes. This study describes texture, microbial composition, and hydrodynamic settings on microbial-rich travertines at Anraku hot spring in Kagoshima Prefecture and Nagayu hot spring in Oita Prefecture.

16S rRNA phylotype analysis of both two samples revealed dominance of a filamentous cyanobacterium closely related to *Microcoleus* sp. that has a high gliding ability. Despite of similar microbial composition, the two samples differ in outer shapes and internal texture, likely depending of the difference in hydrodynamics. A microbial travertine at Anraku hot spring exhibits a conical shape of 5-30 mm in diameter and 10-50 mm in high, which was formed at sidewall of the water discharge where the 55-degree Celsius water was splashing. All peaks of the coniforms inclined 30 degrees to the south corresponding to the direction of mid-day sun light. The surface is dark-green, while the lighter-colored inner part exhibits lamination consisting of alternation of 50 to 200-micron-thick crystal layer and filamentous cyanobacterial layer. The lamination was not daily because this microbe-rich travertine grew only 5 mm during 3 months. SEM image of the surface showed that cyanobacterial filaments were randomly tangled. On the other hand, the microbial travertine at Nagayu hot spring was in a planer form developed slowly flowing (5 cm/sec) water of 35-40 degrees Celsius. Similar to the Anraku one, the surface of the mat was dark-green, but internal texture clearly showed a clear lamination consisting crystalline layers and microbe-rich layers, equally of 250 microns. Sampling throughout a day confirmed that this lamination was daily; crystalline layer was formed during nighttime and microbe-rich layer was formed during the daytime. SEM image of the surface showed extension of the filaments aligned parallel to the flow direction.

Culture experiments in a static water showed that randomly-directed gliding of cyanobacteria formed a tangle of the filaments that generated the starting points of the conical projection (Shepard and Sumner, 2010). On the other hand, such tangles were hardly formed in flowing water that aligned filaments parallel to the flow direction. For the Anraku microbial mat developed under unstable water supply, gliding of cyanobacteria was controlled by their phototactic behavior, and overall directed to the mid-day sunlight. In the Nagayu microbial travertine, the directed filaments formed biofilm during daytime and were covered with precipitated aragonite during nighttime. Thus, regular daily lamina formation resulted from competition between daytime cyanobacterial growth and nighttime inorganic precipitation. Such lamination cannot be formed in the Anraku microbial mat where the water was occasionally splashing.

Conical shaped stromatolites were abundant in Precambrian stromatolites and called *Conophyton*. This study showed that one phylotype of cyanobacteria could make different outer shapes and inner textures of the microbial travertines by reflecting from flow conditions. Building up the geomicrobiological investigation of the modern analogs may lead a new possible interpretation for the stromatolite microbiology and early biosphere.

### References

Shepard, R.N. and Sumner, D.Y. (2010) *Geobiology*, 8, 179-190.

Keywords: stromatolite, cyanobacteria, travertine, microbial mat

## Drying behavior of a rock and its effect on weathering

YOKOYAMA, Tadashi<sup>1\*</sup>, NISHIYAMA, Naoki<sup>1</sup>

<sup>1</sup>Department of Earth and Planetary Science, Osaka University

Rocks near the ground surface undergo cyclic wetting and drying. Dynamic movement of pore water and significant change of chemical composition are induced by drying. Understanding of these processes is important for considering weathering of rocks. We studied the way pore water moves and solute concentration changes during drying. A porous rhyolite, porosity 26% and main pore diameter ranging from 0.1  $\mu\text{m}$  to 260  $\mu\text{m}$ , was used in the experiment. The core was saturated with deionized water, dried at 20 degreeC and weight loss was monitored. The water-saturation (water volume per total pore volume) decreased with elapsed time of drying. Drying rate was relatively constant for the initial period of the experiment (constant-rate stage) and then decreased (falling-rate stage). In order to evaluate the size and chemical composition of pore water under different degrees of drying, we employed centrifugation. It is known that water is progressively extracted from water-bearing rock in order of large to small pores as centrifugal speed increases. Therefore, by extracting pore water with increasing centrifugal speed in incremental steps, we can know the changes in the size of pore water and the solute concentration with progress of drying. The result of the stepwise centrifugation demonstrated that as drying advanced, first larger pores and subsequently smaller pores lost water. Also, solute concentration significantly changed with the progress of drying. Based on the results, we discuss how drying affects dissolution of primary minerals and precipitation of secondary products.

Keywords: drying, weathering, pore water, pore structure

## Effect of water saturation on mineral-water reactive surface area: role of water film

NISHIYAMA, Naoki<sup>1\*</sup>, YOKOYAMA, Tadashi<sup>1</sup>

<sup>1</sup>Dept. Earth & Space Sci., Osaka Univ.

Accurate estimation of mineral-water reactive surface area is essential for quantifying water-rock interaction. Rocks above water tables are usually water-unsaturated, where water and air coexist in pores. There is a possibility that the reactive surface area under unsaturated condition is smaller than that under saturated condition and as the result total amount of reaction becomes smaller. This study aims to investigate the relationship between water saturation and mineral-water reactive surface area.

Fontainebleau sandstone from France, total porosity 7.4%, quartz ~100%, was used. A core was cut from the rock and water-saturation was adjusted to 0, 50, and 100%. Water was run into the sample by applying a constant water pressure. Under an unsaturated condition, only quartz surfaces in contact with water dissolve and the dissolved Si is transported to the outside of the sample by flow of water in pores. At a water saturation  $S$ , the relationship between volume flow rate  $Q(S)$  ( $\text{cm}^3 \text{sec}^{-1}$ ), Si concentration in effluent  $C_{Si}(S)$  ( $\text{mol cm}^{-3}$ ), reactive surface area  $A(S)$  ( $\text{cm}^2$ ), quartz dissolution rate at far from equilibrium  $k_{Qz}$  ( $\text{mol cm}^{-2} \text{sec}^{-1}$ ) (independent of water saturation) is given by  $Q(S) \times C_{Si}(S) = k_{Qz} \times A(S)$ . Therefore, by measuring the flow rate and Si concentration at various water saturations and comparing them with those at saturated condition, variation of reactive surface area with changing water saturation can be evaluated.

Result of experiments showed that the reactive surface area was almost unchanged by the decrease of water saturation. This result indicates that mineral surfaces exposed to air-containing pores were wetted with thick water film, by which dissolution occurred. Furthermore, it suggests that the rate of flushing of dissolved Si to outside of film water was fast enough to keep concentration in film water far lower than equilibrium concentration of quartz. If the flushing rate was small dissolution rate of quartz would have decreased because of the concentration dependence of dissolution rate, but this was not the case. To theoretically evaluate whether or not sufficiently low concentration is maintained by diffusional transport of dissolved element, we derived a theoretical reactive transport model that describes the interplay between dissolution and diffusion through water film. In this model, water film wetting mineral surfaces was assumed to be in equilibrium with relative humidity in pores. It was confirmed that flushing in the film was fast enough to keep sufficiently low Si concentration in the case of our sample. The model shows that the concentration in film water is a function of water film thickness, diffusion length, and mineral properties (dissolution rate, equilibrium concentration, and roughness factor). Thus, effects of water saturation on reactive surface area and dissolution rate differ depending on the type of rock. The model can be applied to predict the relationship of "water saturation"- "reactive surface area"- "dissolution rate" for rocks having various mineral compositions and pore structures.

Keywords: mineral-water reactive surface area, mass transport, water film, rock weathering

## Sulfuric acid of air pollutant and the relation of withering of trees-Prevention from withering by charcoal

OMORI, Teiko<sup>1\*</sup>, Yuzo Yoshiike<sup>2</sup>, Shinobu Okamura<sup>3</sup>, Masato Iwasaki<sup>4</sup>

<sup>1</sup>Department of Science Toho University (former), <sup>2</sup>Department of Science Toho University (former), <sup>3</sup>Department of Science Toho University, <sup>4</sup>A Comprehensive School affiliated with Ashikaga Institute of Technology

Sulfuric acid of air pollutant is carried by wind, and adheres to trees. Only moisture evaporates at the place where the sulfuric acid which dissolved in rain or fog adhered.

Sulfuric acid repeats concentration and accumulation and concentration becomes high.

Sulfuric acid falls to the root of trees with rain. Sulfuric acid acidifies soil. Aluminum and iron of an ingredient of soil become soluble metal salt with the additional sulfuric acid. The absorbed metal ion combines with phosphoric acid of woody layer and becomes compound of insolubility. When phosphoric acid becomes a compound of the insolubility, trees will decline by the same phenomenon as lack of phosphoric acid. In the shortage of phosphoric acid, trees decline regardless of the kind of trees.

The tannin contained in the Japanese oak combines with the iron absorbed from soil, and becomes tannic acid iron.

Tannic acid iron does not have toxicity. As for the declined pine, the amount of exudation of resin decreases. As a result, to the insects which live on the trees of a pine or a Japanese oak as the staple food, environment becomes the optimal and they breed so much.

Bamboo needs much silica to grow. When soil acidifies, silica becomes silicic acid and bamboo can not absorb silicic acid. As a result bamboo declines and withers.

Withering is saved by neutralizing acid soil with the charcoal containing alkaline metal.

Keywords: Air pollution., withers of pine, withere of Japanese oak., Acid soil., tannic acid iron., Phosphoric acid iron

## Changes in lead uptake during transformation of monohydrocalcite to aragonite

MUNEMOTO, Takashi<sup>1\*</sup>, MURAKAMI, Takashi<sup>1</sup>

<sup>1</sup>The university of Tokyo

### INTRODUCTION

Monohydrocalcite is metastable and transformed to aragonite in aqueous solutions [1]. The uptake of phosphate and arsenate, oxyanions, by monohydrocalcite has shown that it depends on the concentration of sorbate whether or not the transformation occurs, and in addition, that the uptake characteristics may vary with the presence or absence of the transformation [2]. This strongly suggests the uptake of oxyanions by monohydrocalcite is not a simple process. On the other hand, there have been few studies for the uptake of cations by monohydrocalcite. We conducted uptake experiments of lead ion by monohydrocalcite to examine changes in uptake behavior of lead ion during transformation of monohydrocalcite to aragonite.

### METHODS

To minimize changes in concentrations of carbonate ions and pH, buffer solutions were equilibrated with atmospheric CO<sub>2</sub> using Na<sub>2</sub>CO<sub>3</sub>, NaHCO<sub>3</sub> and NaNO<sub>3</sub>; the solution pHs were adjusted to pH 8.50, 9.00 and 9.50 by NaOH and HNO<sub>3</sub>. 2 g/L of synthesized monohydrocalcite was added to each solution for the experiments. The transformation kinetics was examined at 1 μM of initial Pb<sup>2+</sup> and pH 8.50, 9.00 and 9.50. The apparent sorption isotherm experiments were conducted at 0.5 to 100 μM of initial Pb<sup>2+</sup> and pH 9.50. The concentrations of Pb were measured at the end of each batch experiment. The durations of the kinetic experiments were up to 15 hours, while all isotherm experiments were carried out for 24 hours.

### RESULTS AND DISCUSSION

Monohydrocalcite was transformed to aragonite in several hours in aqueous solutions. Aragonite increased in amount gradually while monohydrocalcite decreased with time. Monohydrocalcite was almost completely replaced by aragonite in 15 hours. The growth rates of aragonite were almost the same between the three different pH conditions. Before, during and after the phase transformation, the amounts of uptake of Pb<sup>2+</sup> were almost the same at different pH.

The solutions with more than 3 μM of Pb<sup>2+</sup> were supersaturated with respect to cerussite (lead carbonate) which was, however, not identified by X-ray powder diffraction. Therefore, the precipitation of lead carbonate was not predicted in solutions with less than 3 μM of Pb<sup>2+</sup>. Despite the supersaturation in 10 μM initial-Pb<sup>2+</sup> solution, SEM observation of the reacted solid showed that the contrast of BSE image was homogeneous, suggesting Pb was associated with aragonite probably by sorption or coprecipitation. At 100 μM of initial Pb<sup>2+</sup>, fine grains with high contrast were observed by BSE, showing the formation of lead carbonate. Some amount of Pb was considered to be associated with aragonite because of the reasons as follows: (1) the Pb<sup>2+</sup> concentration at the end of the experiment at 100 μM of initial Pb<sup>2+</sup> was about 4 μM, of which the concentration was similar to that for the 5 μM initial-Pb<sup>2+</sup> experiment where about a half of Pb was associated with aragonite and (2) the transformation was completed in 15 hours.

The transformation mechanisms of monohydrocalcite to aragonite are dissolution and precipitation [1]. Depending on the initial Pb<sup>2+</sup> concentrations, portion of Pb forms lead carbonate and some other portion is associated with aragonite after the transformation. Because aragonite increases in amount gradually and because aragonite and cerussite are isostructural to one another, it is possible that the Pb with aragonite forms solid solution during the transformation, which will be clarified in the near future.

### REFERENCE

- [1], Munemoto and Fukushi, 2008, Journal of Mineralogical and Petrological Sciences, 103, 345-349
- [2], Fukushi, et al., 2011, Science and Technology of Advanced Materials, 12, 064702

Keywords: monohydrocalcite, aragonite, transformation, lead

## Iodine uptake by calcium carbonate polymorphs

ANRAKU, Sohtaro<sup>1\*</sup>, Jun HOSHINO<sup>1</sup>, MATSUBARA, Isamu<sup>1</sup>, SATO, Tsutomu<sup>2</sup>, Tetsuro YONEDA<sup>2</sup>

<sup>1</sup>Graduate School of Engineering, Hokkaido University, <sup>2</sup>Faculty of Engineering, Hokkaido University

Iodine has high radioactivity for long term in geological repository, which will be planned as transuranic(TRU) waste repository. Therefore, the immobilization of iodine must be investigated.

Naturally-occurring calcium carbonate, discovered in hyperalkaline spring (pH<12) in Oman, has high distribution coefficient of iodine, especially aragonite. The uptake of iodine on calcium carbonate is effective, because it is possible to form calcium carbonate. Therefore iodine interaction with calcium carbonate must be investigated.

In this study, I conducted some experiments, coprecipitation, adsorption, and desorption, to understand incorporation of iodide and iodate on calcium carbonate, calcite and aragonite.

Coprecipitation was conducted by synthesis of calcium carbonate in the presence of iodide or iodate ion in water. Adsorption was also conducted by synthesis of calcium carbonate, but iodide or iodate ion is not in water. Synthesis calcium carbonate put into iodide or iodate solution (solid/liquid = 400mg/40mL). Iodide and iodate concentrations were 50, 100, 500, 1000, 5000, 10000 ppm respectively both experiments. Then, this solution was open air and stirred with a magnetic stirrer at 25°C for about 24h.

The phase of calcium carbonate was effected by iodate not iodide, and then vaterite and monohydrocalcite were generated instead of calcite and aragonite, respectively. Aragonite has relatively high distribution coefficient than calcite in the experiments of adsorption and coprecipitation in laboratory as the field in Oman. The coprecipitation process of iodide by aragonite was dominant than the adsorption process.

Keywords: calcium carbonate, polymorphs, iodine, adsorption, coprecipitation, natural analogue



## Geochemical reaction modeling of $\text{CaCO}_3$ polymorphs formation at hyperalkaline springs in Oman.

MATSUBARA, Isamu<sup>1\*</sup>, Jun Hoshino<sup>1</sup>, ANRAKU, Sohtarō<sup>1</sup>, SATO, Tsutomu<sup>2</sup>, Teturo Yoneda<sup>2</sup>

<sup>1</sup>Graduate School of Engineering, Hokkaido University, <sup>2</sup>Faculty of Engineering, Hokkaido University

In Japanese transuranic (TRU) waste disposal facilities, <sup>129</sup>I is the most important key nuclide for the long-term safety assessment. Thus, the  $K_d$  values of I to natural minerals are important factor in the safety assessment. However, the degradation of cement materials in the repositories can produce high pH pore fluid which can affect to anion transport behavior. Therefore, it should be necessary to understand behavior of anions such as I<sup>-</sup> under the hyperalkaline conditions.

Natural hyperalkaline spring water (pH>11) has known to generate from the partly serpentinized peridotite in the Oman ophiolite. The spring water is characteristically hyperalkaline, reducing, low-Mg, Si and  $\text{HCO}_3^-$ , and high Ca, while the river water is moderately alkaline, oxidizing, high-Mg and  $\text{HCO}_3^-$ . The mixing of these spring and river water caused the formation of secondary minerals. Naturally-occurring hyperalkaline conditions near the springs in Oman were used as natural analogue for the interaction between cement pore fluid and natural Mg- $\text{HCO}_3^-$  groundwater.

Anraku *et al.* (2009) said that calcite ( $\text{CaCO}_3$ ), aragonite ( $\text{CaCO}_3$ ), hydrotalcite [ $\text{Mg}_6\text{Al}_2\text{CO}_3(\text{OH})_{16}$ ] were observed in the precipitates, and their mineral compositions were varied depending on the difference of sampling points. Moreover, Anraku *et al.* (2009) also said that Iodine can be remarkably fixed in aragonite. If aragonite can also form in disposal condition, safety ratio in the long-term safety assessment will be increased by generation of aragonite.

The main goal of this work is to incorporate the effect of fixing iodine by aragonite into safety assessment. With this aim, we carried out the in-situ synthesis experiment in order to simplify the condition of secondary minerals formation in Oman. Moreover, we tried to model which can express the reaction of the in-situ synthesis experiment.

The in-situ synthesis experiment was conducted by mixing different ratios between spring and river water. The precipitates were synthesized by letting mixing solutions stand for 2 days. The mineralogy of the precipitates was determined by X-ray diffractometer (XRD), scanning electron microscope (SEM). In addition, mass of minerals in the precipitates were obtained by Rietveld method. In the result of this experiment, aragonite formed in all precipitates, and increasing the percentage of river water caused decreasing the percentage of calcite in the precipitates.

The geochemical reaction modeling was performed by using Geochemist's workbench R8.0 based on the result of the in-situ synthesis experiment. Aragonite is well-known as more unstable phase than calcite in earth's surface condition. In equilibrium state, aragonite will not form. Berner (1975) said that Magnesium ion is a inhibitor of calcite growth kinetics. And there is no inhibition of aragonite growth by magnesium ion. Our result showed the same tendency with Berner (1975). Thus, We incorporated Mg inhibition model calculated by Lin and Singer (2009) into our models. the percentage of calcite/aragonite in modeling results corresponded approximately to experimental results. Since generation of aragonite can be possible to calculate, safety ratio in the long-term safety assessment can be increased by generation of aragonite.

Keywords: Calcium carbonate mineral, Polymorphs, Geochemical reaction modeling, Kinetics, Radioactive waste disposal, Natural analogue

## Desorption of Cs from Cs contaminated smectite by major cations

Yuki Yamashina<sup>1</sup>, FUKUSHI, Keisuke<sup>2\*</sup>

<sup>1</sup>School of Natural System, College of Science and Engineering, Kanazawa University, <sup>2</sup>Institute of Nature and Environmental Tehcnology, Kanazawa University

Expandable clay mineral can fix Cs strongly on the inter layer position. However, the fixed Cs can be desorbed by reaction with other cationic species, if the concentrations of the species are especially high. Although it is very important to know the desorption behavior of Cs fixed in expandable clay minerals by major cations, there are very few studies to systematically examine the desorption behaviors. The purposes of the study are (1) to examine the desorption behavior of Cs on smectite by major cations (Na<sup>+</sup>, K<sup>+</sup>, Mg<sup>2+</sup>, Ca<sup>2+</sup> and NH<sub>4</sub><sup>+</sup>) as function of the cation concentrations and (2) to construct the predictive model for the Cs desorption on smectite by the major cations.

Keywords: cesium, smectite, cation exchange, major cations

## Cation Exchange Capacity Measurement for Bentonite by Spectrophotometry

HORIUCHI, Yu<sup>1\*</sup>, TAKAGI, Tetsuichi<sup>1</sup>

<sup>1</sup>Geological Survey of Japan, AIST

The cation exchange capacity (CEC) of bentonite is commonly measured by the method JBAS-106-77, provided by Japan Bentonite Manufacturers Association. JBAS-106-77 instructs the use of ammonium acetate for cation exchange, and recommends the Kjeldahl method for the quantification of ammonium ions. Though this procedure is a general method for the CEC measurement, it is often time-consuming and laborious. There are several other methods for the quantification of ammonia nitrogen, such as spectrophotometry, ionic electrode method, and ion chromatography. Of these methods, the spectrophotometry seems to be most favorable for the CEC measurement, in the point of accuracy, simplicity and quickness. In this study, we have tried to experiment spectrophotometry by using indophenol color development for attempting of convenient CEC measurement. Indophenol represents blue color, which is generated by the reaction of ammonium ions with phenol and hypochlorite.

As a result of the experiment, color development of samples started immediately after the mixture of reagent. The absorbance had stabilized after 4-5 hours, without regard to the concentration of ammonia nitrogen. The CEC value of standard bentonite, measured by the absorbance after 5 hours, represented lower values than expected value of this sample by the Kjeldahl method. This inconsistency is probably resulted from inappropriate conditions of color development, such as pH. In the future, it is necessary to improve the accuracy and reproducibility of this CEC measurement.

## Origin of manganese oxide in cold spring, Saga Prefecture.

TAKASHIMA, Chizuru<sup>1\*</sup>, HIGASHI, Yuka<sup>1</sup>, MORI, Taiki<sup>1</sup>, OKUMURA, Tomoyo<sup>2</sup>

<sup>1</sup>Faculty of Culture and Education, Saga Univ., <sup>2</sup>Graduate School of Social and Cultural Studies, Kyushu Univ.

Manganese oxide plays an important role in material cycling and has been reported from fresh water, hot springs and deep-sea hydrothermal vents (e.g., Mita et al., 1994; Fitzgerald and Gillis, 2006). In this study, we focused on manganese oxide in cold spring and discussed about the origin and the water chemistries.

Study site is Hiramatsu cold spring in Saga City, Ssga Prefecture, and is used for bathing at Hiramatsu welfare center located ~60 m from the spring. The water emit from a well naturally and is first stored in a tank close to the spring (tank 1). Then, the water in tank 1 is transported by pomp to another tank next to the welfare center (tank 2) and used in bathtub after heating. Manganese-rich precipitate was prominent at the tank 2, but also seen in the spring, tank 1, and the bathtub,

We collected water samples from the spring, tank 1 and tank 2. They were used for analysis of water chemistries with XRF and oxygen and carbon isotopic ratio with a mass-spectrometer. For the manganese precipitate collected from the tank 2, we observed textures and microbes with optical and fluorescence microscope and SEM. Moreover, identification of mineralogy was performed by XRD.

The water at the spring was about 18 degrees and shows neutral or faintly alkaline pH. The springwater was microaerophilic, containing dissolved oxygen (DO) of about 0.6 mg/L. It is rich in Mg (about 50 mg/L), Ca (about 35 mg/L), Na (about 30 mg/L), Cl (about 17 mg/L). Mn concentration was about 2 mg/L, and Fe was hardly detected (below 0.1 mg/L). Concentration of Mn decreased from the vent to tank 2. Oxygen isotopic values were -6.9 to -6.0 permill and consistent with a value of meteoric water in north Kyushu area (-7.0 to -6.0 permill; Mizota and Kusakabe, 1994). Low carbon isotopic value (-17.6 permill) of the dissolved inorganic carbon indicates contribution of organic carbon in soil.

Manganese oxide of black to dark brown in color was very soft and unconsolidated. Mineralogy analysis conformed that it was manganese oxide, but shows a broad peak indicating the amorphous MnO<sub>2</sub>. The precipitate contained numerous brown colored filaments of 3-4 micrometers in width, which were covered with mineral precipitates. This showed that bacteria induced precipitation of MnO<sub>2</sub>. Inorganic oxidation reaction of manganese under neutral pH is slow even in an O<sub>2</sub> saturated setting, but is largely enhanced by bacterial activity (Zhang et al., 2002). It is known *Psuedomonas* sp. and *Leptothrix discophora* as manganese oxide bacteria, but at present, type of bacteria in this manganese oxide are not specified. Further examination is needed to identify the bacteria with detailed observation and phylotype analysis.

### [References]

Fitzgerald, C.E. and Gillis, K.M. (2006) Hydrothermal manganese oxide deposits from Baby Bare seamount in the Northeast Pacific Ocean. *Marine Geology*, 225, p. 145-156.

Mita, N., Maruyama, A., Usui, A., Higashihara, T and Hariya, Y. (1994) A growing deposit of hydrous manganese oxide produced by microbial mediation at a hot spring, Japan. *Geochemical Journal*, 28, p. 71-80.

Mizota, C. and Kusakabe, M. (1994) Spatial distribution of dD-d<sup>18</sup>O values of surface and shallow groundwaters from Japan, south Korea and east China. *Geochemical Journal*, 28, p.387-410.

Zhang, J., Lion, L.W., Nelson, Y.M., Shuler, M.L., and Ghiorse, W.C. (2002) Kinetics of Mn(II) oxidation by *Leptothrix discophora* SS1. *Geochimica et Cosmochimica Acta*, 65, p.773-781.

Keywords: Manganese oxide, bacteria, cold spring

## Estimation of chemical weathering rates using a process-based chemical weathering model

NOZU, Taichi<sup>1\*</sup>, TAJIKA, Eiichi<sup>2</sup>

<sup>1</sup>Dept. EPS, Sch. Sci., Univ. Tokyo, <sup>2</sup>Dept. Complex. Sci. Eng., Univ. Tokyo

Chemical weathering of silicate minerals has been recognized as one of the most important processes in the long-term geochemical cycles in the Earth system. However, field-based studies on different spatial-scale watersheds have shown that the chemical weathering rates are different according to the scale of observations. Long-term mineral dissolution experiments and compilation of chemical weathering rates estimated for different weathering durations suggested that the chemical weathering rates decline significantly with time. The discrepancy may be explained as a sum effect of several phenomena such as increase in surface roughness with time and difference in reaction affinities between natural and experimental conditions.

We are developing a process-based chemical weathering model to study behaviors of the geochemical cycle system in response to changes in modern- and paleo-environment. This model consists of soil physics (heat, moisture, and gas transport) modules, chemical reaction (mineral dissolution/precipitation and aqueous speciation) modules, and a simplified soil biological activity module. We consider difference and variation in hydraulic parameters depending on soil texture and moisture content. The model has been applied to several different small (< 10 km<sup>2</sup>) watersheds to verify the model to reproduce major ion concentrations of modern streams. We introduced a free parameter which represents a ratio of field-scale weathering rate to mineralogical dissolution rate to fit the observational data. Sensitivity analyses show that riverine ionic concentrations of base cations are well reproduced from the model by tuning this parameter alone. This parameter may represent erosional effect which, in turn, controls age of the weathering environment. That is, the time dependency of silicate weathering can explain the difference in this parameter. The obtained parameter is also comparable with the ratio of the effective surface area to the BET surface area estimated in previous studies. Methods of determination of the effective surface area from environmental parameters such as an erosion rate and lithology will be discussed.

Keywords: chemical weathering, effective surface area, numerical model

## Rapid change of sedimentary environments in ca. 13Ma at Hokuroku area: mineralogical and geochemical studies on pyrite

ENDO, Misato<sup>1\*</sup>, Ryoichi Yamada<sup>1</sup>, Takeshi Kakegawa<sup>1</sup>

<sup>1</sup>Graduate School of Science, Tohoku Univ.

Previous study suggested that the bottom water locally become anoxic after the formation of Kuroko deposits in the Hokuroku district, Akita in Japan (Komuro et al., 2004). However, the temporal and spatial distribution of anoxic water during 15 to 10 Ma are still poorly understood. Anoxic bottom water may be a critical factor in the initial preservation of volcanogenic massive sulfide deposit (VMS) (Eastoe and Gustin, 1996). Therefore, the importance exists as to if the Kuroko deposits were also preserved in anoxic conditions or not.

Size distribution of pyrite framboids in carbonaceous sedimentary rocks is one indicator to identify the presence of anoxic ocean water. Carbonaceous sedimentary rocks, which age range from 15 to 10 Ma, are available in the Hokuroku district. In addition to age distribution, the same-aged carbonaceous sedimentary rocks are largely extended. Therefore, those carbonaceous sedimentary rocks have potential to examine temporal and spatial distribution of anoxic water in the past Hokuroku district.

In this study, geological, geochemical, and mineralogical investigations were carried out on mudstones in the Hokuroku district. In particular, the size distributions of pyrite framboids were analyzed using SEM. The mudstones from M3, M2 Ma and M1 were collected from outcrops in the large area of the Hokuroku district. The M3 mudstone, which age is most likely between 15 to 14 Ma, was deposited before the formation of Kuroko deposits. M2 mudstone was deposited soon after Kuroko hydrothermal activity (ca.14 to 13 Ma). M1 and M1 mudstones, which ages are ranging from 13 to 10 Ma were deposited with no relation to Kuroko hydrothermal activity.

Detailed size analyses showed that mean sizes of pyrite framboids in the M2 mudstones (5.0 to 5.2 micro meters) were smaller than those of M3, M1 and M1 mudstones (5.0 to 9.7 micro meters). The standard deviation of pyrite framboids in the M2 (2.0), were also smaller than those of others (2.4 to 4.2). These results above indicate that M2 mudstones were deposited under euxinic conditions, and M3, M1 and M1 mudstones were deposited under oxic conditions. The examined M2 mudstones were collected both near and far from the ore bodies and all show the same size distribution of framboidal pyrite. This suggests that anoxic water were rather widespread at the bottom of the Hokuroku ocean between 14 to 13 Ma. On the other hand, anoxia of bottom ocean water only restricted during sedimentation of M2 mudstones. The total range of sulfur isotopic compositions of pyrites were range from -44 to -15 per mil. In particular, the sulfur isotope compositions of pyrites in M2 were range from -37 to -34 per mil. Such light values indicate microbial sulfur cycling by sulfate-reducing, sulfur-oxidizing and/or sulfur-disproportionating bacteria in the anoxic water column. On the other hand, S(pyrite)/C(organiCs) in M2 mudstone is not high compared to Black Sea sediments, which deposited in euxinic conditions and redox boundary reached to photic zone. Those facts indicate that euxinic bottom water at the pale-Hokuroku ocean were created by microbial activities, not submarine hydrothermal activities. The anoxic water at this age was limited at the bottom of deep ocean and did not reached to photic zone, so that the magnitude of microbial productivities (and pyrite precipitation) at redox boundary were limited.

On the other hand, the sulfur isotope compositions of pyrites in the upper part of M1 and M1 range from -30 to -15 per mil. M1 mudstones contain the secondary pyrite (e.g., pyrite overgrowth on primary framboidal pyrite). Such secondary pyrite often contain unusual amounts of Mn. Texture and chemistry of secondary pyrite suggest that those were formed during late diagenetic stage by dissolving and reprecipitating primary framboidal pyrite. Such diagenetic process, accompanied with change of clastic sediments and sedimentation rates, may affected on sulfur isotope compositions of M1 and M1.

Keywords: pyrite framboids, Kuroko deposits, bacterial activity, anoxic

## Microbial sulfate reduction within the Iheya North subseafloor hydrothermal system constrained by quadruple sulfur isoto

AOYAMA, Shinnosuke<sup>1\*</sup>, NISHIZAWA, Manabu<sup>2</sup>, TAKAI, Ken<sup>2</sup>, UENO, Yuichiro<sup>1</sup>

<sup>1</sup>Tokyo Institute of Technology Department of Earth and Planetary Sciences Tokyo Institute of Technolo, <sup>2</sup>JAMSTEC

Subseafloor hydrothermal system may host active and abundant microbial community. Sulfate reduction may be one of the dominant microbial metabolisms among the subseafloor ecosystem. In order to demonstrate and quantify the potential sulfate reducing activity, we analyzed sulfur isotopes ( $^{32}\text{S}/^{33}\text{S}/^{34}\text{S}/^{36}\text{S}$ ) of pore water sulfate extracted from core samples at the Iheya North hydrothermal system in the Okinawa drilled by CHIKYU, 2009 (IODP Leg 331). After drilling, core samples were divided into several sections. Then, pore water was extracted on board, and stored with cadmium chloride for fixing hydrogen sulfide. In our laboratory, the samples were first divided into sulfide precipitate and supernatant liquid by centrifugation. Then, dissolved sulfate was precipitated as  $\text{BaSO}_4$  by addition of barium chloride into the supernatant liquid. After weighing, the barium sulfate was converted into silver sulfide and subsequently sulfur hexafluoride, which was purified by GC and then introduced into mass spectrometer (MAT253) through newly developed microvolume inlet for precisely determining quadruple sulfur isotopic composition.

Based on pore water chemistry and temperature profile, the subseafloor environment are divided into Unit-1, -2 and -3 with depth below surface. In Unit-1 (0-10 mbsf), fresh seawater is circulated, whereas in Unit-3 (>40 mbsf), hot hydrothermal fluid (>150°C) is stored below anhydrite cap. The Unit-2 is the mixing zone between the hydrothermal fluid and seawater.

We found that the  $\delta^{34}\text{S}$  value of sulfate in the mixing zone was higher than those expected by simple mixing between seawater sulfate in Unit-1 (-20 permil) and the hydrothermal component in Unit-3 (-16 permil). The observed  $^{34}\text{S}$ -enrichment and decreased sulfate concentration suggest sulfate reduction took place in this hydrothermal system. Based on our model calculation assuming the mixing and reduction, apparent isotope effect for  $^{33}\text{S}$ ,  $^{34}\text{S}$  and  $^{36}\text{S}$  are estimated to be -16.5 permil, -32.2 permil and -62.5 permil, respectively. These large fractionations together with slight  $\text{D}^{33}\text{S}$  enrichment and  $\text{D}^{36}\text{S}$  depletion all suggest that the sulfate reduction is microbial and not thermochemical process. Our numerical simulation also indicates that the sulfate is reduced before mixing with high temperature fluid, probably within the recharge zone of seawater. Based on these results, we will discuss microbial sulfur cycling in this subseafloor environment.

Keywords: Microbial sulfate reduction, quadruple sulfur isotope, subseafloor hydrothermal system, Iheya North hydrothermal system in the Okinawa

## Impact Chemical Evolution Processes for Simple Amino Acids (Glycine and Alanine) Formed by Oceanic Impact

UMEDA, Yuhei<sup>1\*</sup>, FUKUNAGA, Nao<sup>1</sup>, SEKINE, Toshimori<sup>1</sup>, FURUKAWA, Yoshihiro<sup>2</sup>, KAKEGAWA, Takeshi<sup>2</sup>, Kobayashi Takamishi<sup>3</sup>, NAKAZAWA, Hiromoto<sup>3</sup>

<sup>1</sup>Graduate School of Science, Hiroshima University, <sup>2</sup>Graduate School of Science, Tohoku University, <sup>3</sup>National Institute for Materials Science

The biomolecules on Earth are thought either to have come from the extraterrestrial parts carried with flying meteorites or to have been formed on Earth from the inorganic materials through given energy. From the standpoint to address the importance of impact energy, it is required to simulate experimentally the chemical reactions during impacts, because violent impacts may have occurred 38-40 years ago to create biomolecules initially. Shock reactions between ocean and meteoritic constitutions can induce locally reduction environment to form bioorganic molecules such as amino acid.

We need to know possible processes how the chemical evolution proceeds further by impacts and how complicated biomolecules are formed. In this study we prepared aqueous solutions of the two simplest amino acids (glycine and alanine) labeled by <sup>13</sup>C and investigated the reactions. Shock recovery experiments were carried out with a propellant gun. Sample of aqueous solution immersed in olivine powders sealed in a stainless steel container was used as a target. The sample space has air gap behind the mixture of olivine and solution. In some shots we added ammonia solution and so on to model the old ocean composition. The recovered samples were analyzed with LC/MS for water soluble components and XRD and TEM for solids. The analytical results indicate the formations of alanine from glycine, glycine from alanine, and amines from the both and that the residual glycine and alanine in each solution are very small less than 1%. There is no evidence for formation of complicated amino acids even if benzene was added. The starting olivine particles became fine-grained and some grains had reaction rims of hydration. According to the present results, simple amino acids of glycine and alanine can change one another, but they decompose amines and others mostly. So, these results imply not only that the impact-induced process is not so simple to proceed the chemical evolution just to one way, but also that there are complicated and multi-process ways. In meteorite impacts, it also must be taken into account the heterogeneous distribution of impact energy in an impact that may cause a significant effect on the chemical evolution.



## Chirality change of valine by marine bolide impacts

TAKASE, Atsushi<sup>1\*</sup>, SEKINE, Toshimori<sup>1</sup>, FURUKAWA, Yoshihiro<sup>2</sup>, KAKEGAWA, Takeshi<sup>2</sup>, Takamichi Kobayashi<sup>3</sup>, NAKAZAWA, Hiromoto<sup>3</sup>

<sup>1</sup>Graduate School of Science, Hiroshima University, <sup>2</sup>Graduate School of Science, Tohoku University, <sup>3</sup>National Institute for Materials Science

The chirality of terrestrial amino acids consisting of biomolecules is only L-type. In order to make clear the origin of life from the standpoint that biomolecules are formed by oceanic impacts of meteorites, it is crucial to determine the chirality change of amino acids through impact process that have been considered to have occurred at early Earth. Each aqueous solution (~100 mmole/l) of L- and D-valine was prepared separately and used as reactants. Samples after shock recovery experiments on mixtures of powdered olivine and the solution were analyzed by LC/MS for the contents of L- and D-valines. The present results indicate that valine survives significantly (~10%) and that the aqueous L- and D-valines transform partially (~5%) to D- and L-valines, respectively. Although further studies need to define how the final chirality changes by shock processes, marine bolide impact may have significant effects on the chirality and the chemical evolution of biomolecule.

## Causes of recent increased aeolian dust productions over East Asia - An analysis using meteorological observatory data

KUROSAKI, Yasunori<sup>1\*</sup>, SHINODA, Masato<sup>1</sup>, MIKAMI, Masao<sup>2</sup>

<sup>1</sup>Arid Land Research Center, Tottori University, <sup>2</sup>Meteorological Research Institute

Production of aeolian dust (i.e., wind erosion) depends on aeolian erosivity and erodibility. The erosivity is an ability of wind to cause wind erosion, and it can be represented by one parameter, which is wind friction speed or simplistically wind speed. On the other hand, the erodibility is characterized as the sensitivity of a surface to wind erosion, which is influenced by an infinite number of soil and land surface characteristics, particularly the soil particle size distribution, soil water content, soil freeze/thaw processes, snow cover, vegetation coverage, vegetation type, and we do not clarify most relations between these parameters and erodibility. Even though all of these will be clarified, we will still have difficulties in monitoring the all erodibility factors. The above means monitoring erosivity is relatively easy but monitoring erodibility is difficult.

We can recognize the minimum wind speed initiating an dust production (hereafter, threshold wind speed) as an index of erodibility. Estimations of threshold wind speed have been conducted by a combination of anemometers and devices which measure instantaneous soil particles motions, such as SENSIT (Stout, 2004, Earth Surf. Processes Landforms) and SPC (Mikami et al., 2005, J. Geophys. Res.). However long-term erodibility monitoring by such devices in a broad area is not realistic due to problems of manpower and fund.

We can monitor a dust production in a broad area for a long term using synoptic data whose observation is made at meteorological observatories, which are widely distributed in the world. A meteorological observation is conducted at every 3-hour at many of synoptic observatories. A dust production is recorded in a present weather observation. Regarding erosivity, we have a wind speed observation. However, we have no observation of erodibility.

In this presentation, we will show a methodology of statistical estimate of threshold wind speed (Kurosaki et al., 2011, Geophys. Res. Lett.). We will show dust production frequency, strong wind frequency, and 5-percentile of threshold wind speed on April for 1990s (1990-1999) and 2000s (2000-2009) over East Asia, and we will discuss the contribution of erosivity and erodibility on changes in dust production from 1990s to 2000s from changes in strong wind frequency and 5-percentile of threshold wind speed. Here, a strong wind is defined as a wind whose wind speed exceeds 5-percentile of threshold wind speed on April for 1970-2009. We will also show analyses of precipitation for June-August (hereafter, summer precipitation) and annual maximum NDVI (Normalized Difference Vegetation Index) in order to examine dead-leaf hypothesis (Shinoda et al., 2010, SOLA). In this hypothesis, the precipitation amount during the vegetation growing season predominantly controls plant production in summer, the vegetation in summer remains as dead leaves until spring of the following year, and consequently the dead leaves chiefly control the erodibility in spring. Our main results are as below:

1. The dust production frequency increased at many observatories in Mongolia, Inner Mongolia, and northeastern China, whose land cover types are grassland and cultivated land, from the 1990s to the 2000s due to changes in erodibility.
2. We have some observatories where the dust production frequency increased for the period in the Gobi Desert in China and a western part of the Loess Plateau, whose land cover type is desert, due to changes in erosivity.
3. Both summer precipitation and annual maximum NDVI decreased at some observatories in Mongolia, but no such relationship is seen in other regions. This result suggests that the dead-leaf hypothesis can be applied to such observatories in Mongolia, but not to the other regions.

Keywords: aeolian dust, Asian dust, wind erosion, erosivity, erodibility

## Precipitation rate and isotopic composition of calcium carbonate under conditions induced by degassing of carbon dioxide

KANO, Akihiro<sup>1\*</sup>, Tomoyo Okumura<sup>1</sup>

<sup>1</sup>Kyushu University

It has been well known that degassing of carbon dioxide increases the saturation state and induces precipitation of calcium carbonate. Representative natural examples of this phenomenon are fluvial tufa in a limestone area, and travertine in carbonate hot-spring environments. These two examples largely differ in the precipitation rate. The difference is likely related with the differences in equilibrate partial pressure of carbon dioxide, alkalinity, and calcium concentration, however it has not been fully understand with a theoretical principle. In general, the carbonate precipitation has been treated as adjunction of carbonate and calcium ions on the mineral/water interface, which was often formulated by activity product of the two ions. The previous formulas are consistent with the rates in tufa environments, but fail to reproduce high precipitation rates of the travertines.

This study will propose a new rate formula based on the sum of chain-reactions, in which the degassing induces the carbonate precipitation. A prominent feature of this is that three ions (bicarbonate, hydroxide, and calcium) are captured on the mineral surface. The formulated rate is proportional to the product of the calcium carbonate saturation and the carbon dioxide partial pressure, and well reproduces the actual precipitation rates of tufas and travertines. In addition, the proposed model is consistent with an apparent disequilibrium of oxygen isotopic composition of travertine, which is variable with pH. The model can be more comprehensive than the previous ones in terms of reproducing the overall phenomena of carbonate precipitation.

Keywords: travertine, tufa

## Change of host phase of REE and preservation of REE pattern during the diagenesis of marine sediments

TAKAHASHI, Yoshio<sup>1\*</sup>

<sup>1</sup>Hiroshima University

Relative abundances of rare earth elements (REE) in geological materials are used widely to investigate geochemical problems such as the origins of sedimentary rocks and REE behavior during processes such as weathering and diagenesis. One of the REE, cerium (Ce), can exist in either trivalent or tetravalent form depending on the redox condition. Thus, knowledge of the oxidation state of Ce in rocks and minerals could potentially be used to constrain the redox states of past and present geological environments. In this study, we examined validity of REE pattern as geochemical indicators reflecting sedimentary paleoenvironment.

For this aim, we discussed the behavior of REE under diagenetic environment by using Ce and Mn distributions in sediments, and oxidation states of Ce and Mn determined in X-ray absorption near edge structure (XANES). Sediment core samples used in this study were recovered from North Pacific at Site 1179, ODP Leg 191. Sediment at these core sites consists of siliceous ooze, clay, and thin volcanic ash layer. According to XRF data, the concentration depth profiles of Fe and Mn show that they have high concentration peaks. Manganese is accumulated at 0.20 m, and then decreases toward deep due to reductive dissolution of MnO<sub>2</sub>. The oxidation state of Mn from 0.60 m to 7.18 m is mostly divalent, which is consistent with the low concentration of Mn layer. Marine ferromanganese nodule is known to have a high absorption capacity for REE. Among the REE, Ce tends to accumulate in Mn oxide due to oxidation from soluble Ce<sup>III</sup> to insoluble Ce<sup>IV</sup>. Cerium concentration in sediments is relatively constant from top to bottom of the core, but Mn concentration is not. These results imply that the host phase of Ce changed from Mn-oxides to the other phase.

We confirmed that host phase of Ce changed from Mn oxide to phosphate based on the chemical leaching experiments. Additionally, positive Ce anomaly were observed in both Mn and P phases determined by laser ablation (LA)-ICP-MS, suggesting that the anomaly was conserved during change in the host phase of Ce. Micro-XANES study also showed that Ce in Mn oxides is tetravalent, but trivalent in apatite found at the depths of 0.70 m and 0.80 m.

Overall, the shapes of REE patterns were similar from the surface to the depths studied here, though the host phase of REE changed from Mn oxides to phosphate. Thus, the phosphate having high affinity for REE is important to keep the initial REE pattern during the diagenesis.